Cell, Vol. 117, 95–106, April 2, 2004, Copyright ©2004 by Cell Press

Phosphorylation by the β-Catenin/MAPK Complex Promotes 14-3-3-Mediated Nuclear Export of TCF/POP-1 in Signal-Responsive Cells in *C. elegans*

Miao-Chia Lo,[1] Frédérique Gay,[2] Raanan Odom,[1] Yang Shi,[2] and Rueyling Lin[1,*]
[1]Department of Molecular Biology
University of Texas Southwestern Medical Center
6000 Harry Hines Boulevard
Dallas, Texas 75390
[2]Department of Pathology
Harvard Medical School
77 Avenue Louis Pasteur
Boston, Massachusetts 02115

Summary

In *C. elegans* embryos, a Wnt/MAPK signaling pathway downregulates the TCF/LEF transcription factor POP-1, resulting in a lower nuclear level in signal-responsive cells compared to their sisters. Although the β-catenin WRM-1 is required for POP-1 downregulation, a direct interaction between these two proteins does not seem to be required, as the β-catenin-interacting domain of POP-1 is dispensable for both POP-1 downregulation and function in early embryos. We show here that WRM-1 downregulates POP-1 by promoting its phosphorylation by the MAP kinase LIT-1 and subsequent nuclear export via a 14-3-3 protein, PAR-5. In signal-responsive cells, we also detect a concurrent upregulation of nuclear LIT-1 that is dependent on Wnt/MAPK signaling. Our results suggest a model whereby Wnt/MAPK signaling downregulates POP-1 levels in responsive cells, in part by increasing nuclear LIT-1 levels, thereby increasing POP-1 phosphorylation and PAR-5-mediated nuclear export.

Introduction

The highly conserved Wnt/Wingless family of secreted proteins regulates many aspects of animal development by inducing changes in gene transcription within responding cells. The transcriptional changes induced by Wnt signaling are mediated by the TCF/LEF family of HMG box-containing proteins. The events that follow Wnt signal reception and lead, via TCF/LEF, to transcriptional changes have been extensively studied (see reviews by Polakis, 2000; Pandur and Kuhl, 2001). Most studies support the model in which Wnt signaling stabilizes β-catenin, allowing β-catenin to enter the nucleus, where it complexes with the TCF/LEF transcription factor and activates transcription. In the absence of Wnt signaling, β-catenin associates primarily with the cell membrane, where it contributes to adherens junctions and is degraded in the cytoplasm (see review by Bullions and Levine, 1998).

In the nematode *C. elegans*, a similar canonical Wnt signaling pathway has been identified and shown to regulate postembryonic cell fate decisions through the TCF/LEF transcription factor POP-1. However, in the *C. elegans* early embryo, POP-1 appears to be regulated by a noncanonical Wnt signaling pathway. In four-cell embryos, a signal from the P2 blastomere to its adjoining blastomere EMS is required for the posterior daughter of EMS, E, to adopt an endoderm fate (Figure 1A; Rocheleau et al., 1997; Thorpe et al., 1997). Genetic and molecular analyses have identified genes required for this endoderm induction as components in the Wnt and MAP kinase (MAPK) signaling pathways. These include MOM-1/Porcupine (Rocheleau et al., 1997), MOM-2/Wnt (Rocheleau et al., 1997; Thorpe et al., 1997), MOM-5/Frizzled (Rocheleau et al., 1997; Thorpe et al., 1997), WRM-1/β-catenin (Rocheleau et al., 1997), LIT-1/MAPK (Kaletta et al., 1997; Ishitani et al., 1999; Meneghini et al., 1999; Rocheleau et al., 1999), and MOM-4/MAPKKK (Ishitani et al., 1999; Meneghini et al., 1999; Shin et al., 1999). POP-1 is detected at a lower level in the nucleus of E compared to its anterior sister, MS, and this low POP-1 level requires P2-to-EMS Wnt/MAPK signaling (Lin et al., 1995; Rocheleau et al., 1997; Thorpe et al., 1997). In *pop-1* mutant embryos, MS adopts the fate of E and produces endoderm, suggesting (1) that POP-1 represses endoderm fate in MS and (2) that Wnt/MAPK signaling downregulates the POP-1 level in the Wnt-responsive blastomere E, thereby allowing the endoderm fate.

The asymmetric nuclear POP-1 pattern extends beyond the MS/E sister blastomeres, with higher POP-1 levels in the anterior nuclei of all anterior-posterior (A-P) divisions throughout early embryogenesis (will be referred to hereafter as POP-1 nuclear asymmetry; Lin et al., 1998). We and others have shown that POP-1 is also responsible for the A-P fate difference in many pairs of sisters (Lin et al., 1998; Schroeder and McGhee, 1998; Hermann et al., 2000). Although the signaling source for POP-1 nuclear asymmetry outside of the MS/E blastomere pair remains unclear, it appears that at least some components in the Wnt/MAPK pathway downregulate POP-1 in the posterior cells of A-P divisions throughout the early embryo (Lin et al., 1998; Rocheleau et al., 1999).

Consistent with a role regulating POP-1 nuclear asymmetry in vivo, LIT-1 MAPK can phosphorylate POP-1 in vitro (Rocheleau et al., 1999). When LIT-1, WRM-1, and POP-1 were cotransfected into mammalian tissue culture cells, POP-1 was seen to redistribute from the nucleus to the cytoplasm in a proportion of transfected cells (Rocheleau et al., 1999). These results suggest that phosphorylation of POP-1 by LIT-1 regulates POP-1 nucleocytoplasmic redistribution in mammalian cells. A similar regulation may function in *C. elegans* embryos, as estimates of combined nuclear and cytoplasmic POP-1 in MS and E were similar, suggesting nucleocytoplasmic redistribution as a mechanism for the observed POP-1 nuclear asymmetry (Maduro et al., 2002). Although the β-catenin WRM-1 is required for POP-1 nuclear asymmetry, the β-catenin-interacting domain of POP-1 is dispensable for both its nuclear asymmetry and function in early embryos, making it unlikely that

*Correspondence: rueyling.lin@utsouthwestern.edu

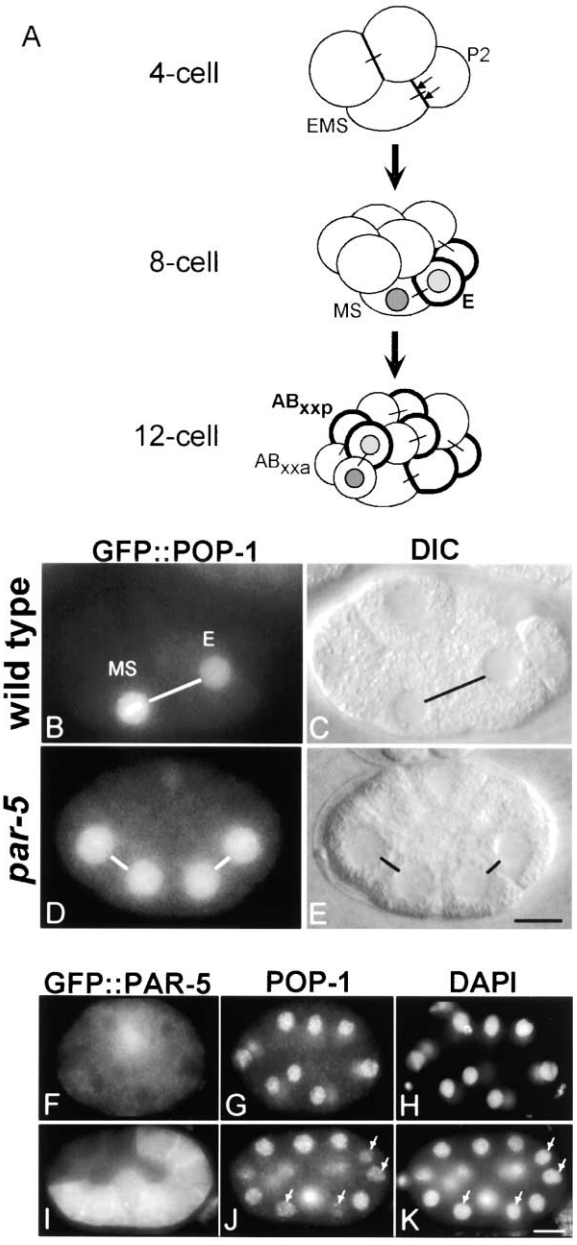

Figure 1. PAR-5 Function Is Required for POP-1 Nuclear Asymmetry in Early Embryos

(A) Schematic diagrams of early *C. elegans* blastomeres. Posterior sisters of A-P divisions, which are indicated by short lines, are shown in thick outline. Names of blastomeres relevant to this study are listed. ABxxa and ABxxp refer to anterior and posterior, respectively, great granddaughters of the AB blastomeres. Nuclei of MS, E, ABala, and ABalp are shown as closed circles inside cells. Different shadings represent different levels of nuclear POP-1, with the darker gray being higher. All graphs are shown with anterior to the left and dorsal up.

(B–E) Micrographs showing GFP::POP-1 fluorescence (B and D) and DIC images (C and E) of eight-cell wild-type (B and C) and *par-5(it55)* (D and E) embryos. Black and white lines in each panel indicate sister blastomeres whose nuclei are equally focused at that particular focal plane.

(F–K) Immunofluorescence micrographs showing POP-1 staining with mabRL2 (G and J) and DAPI (H and K) in *par-5(it55)* mutant embryos with (I, J, and K) or without (F, G, and H) the $P_{med\text{-}1}$*gfp::par-5* transgene. Arrows in (J) and (K) point to nuclei with low levels of nuclear POP-1. Scale bar, 10 μm.

direct binding between POP-1 and WRM-1 regulates POP-1 subcellular localization (Maduro et al., 2002).

We show in this manuscript that asymmetric nuclear POP-1 levels between A-P sisters require a conserved 14-3-3 protein encoded by the *par-5* gene as well as the exportin CRM-1. We demonstrate a physical interaction between POP-1 and PAR-5 that requires both LIT-1 and WRM-1. We identify five potential phosphorylation sites important for POP-1 nuclear asymmetry and show that at least two of these sites are phosphorylated in vivo. In addition, we show that the LIT-1/WRM-1 complex promotes POP-1/PAR-5 interaction and POP-1 nuclear export via phosphorylation of at least a subset of these sites in POP-1. Finally, we show that the nuclear levels of LIT-1 kinase are also asymmetric between A-P sisters in early embryos in a pattern reciprocal to that of POP-1. This LIT-1 asymmetry is regulated by upstream components of the Wnt/MAPK pathway. These results together support the model that Wnt/MAPK signaling results in a high nuclear level of LIT-1 kinase in the signal-responsive cells, leading to POP-1 hyperphosphorylation, POP-1/PAR-5 interaction, and subsequent POP-1 nuclear export.

Results

GFP::POP-1 Nuclear Asymmetry Requires PAR-5, a 14-3-3 Protein

The GFP::POP-1 produced from the transgene $P_{med\text{-}1}$*gfp::pop-1* recapitulates the POP-1 nuclear asymmetric pattern observed with POP-1 antibody staining (Figures 1B and 1C), and the transgene rescues the *pop-1(zu189)* mutant phenotype (Maduro et al., 2002; Gay et al., 2003). To identify additional proteins functioning in the regulation of POP-1 nuclear asymmetry, we introduced the $P_{med\text{-}1}$*gfp::pop-1* transgene into various mutant backgrounds shown to be defective in embryonic polarity (R.O. and R.L., unpublished data). One of the mutants that resulted in the abolishment of POP-1 nuclear asymmetry in early embryos was *par-5(it55)*.

Mutations in *par-5* result in defects in the partition of cytoplasmic contents and timing of divisions in early blastomeres (Morton et al., 2002). The *med-1* promoter is transcribed ubiquitously in the *par-5(it55)* mutant embryos, resulting in the ubiquitous expression of GFP::POP-1 starting at the eight-cell stage. The level of nuclear GFP::POP-1 is equal between sisters, regardless of their division axes (100%, $n = 30$; Figures 1D and 1E). When these eight cells divide, each produces two daughters with equal levels of nuclear GFP::POP-1 (100%, $n = 30$; data not shown), suggesting that PAR-5 is required for GFP::POP-1 nuclear asymmetry in early embryos. This defect is specific to *par-5(it55)* embryos and not observed in other partition-defective mutants (R.O. and R.L., unpublished data). We also detect a similar but less penetrant defect in the nuclear asymmetry of the endogenous POP-1 in *par-5(it55)* embryos when assayed with the monoclonal antibody mabRL2 (69%, $n = 32$; Figure 1G). The asymmetric GFP::POP-1 pattern is gradually reestablished in *par-5(it55)* embryos after the 16-cell stage and is observed in almost all A-P sisters after the 64-cell stage ($n > 100$; data not shown).

The *par-5* gene, also known as *ftt-1*, encodes one of

the two closely related *C. elegans* 14-3-3 proteins and is expressed maternally (Wang and Shakes, 1997; Morton et al., 2002). 14-3-3 proteins are evolutionarily conserved proteins that have been shown to regulate diverse cellular processes via interaction with different binding partners (see review by Fu et al., 2000). The second *C. elegans* 14-3-3 protein, FTT-2, is expressed zygotically after the eight-cell stage (Wang and Shakes, 1997). Gradual restoration of POP-1 nuclear asymmetry in *par-5(it55)* mutant embryos is likely due to the expression of FTT-2. However, because *par-5* and *ftt-2* share nearly identical sequences, we have been unable to prove this point by depleting FTT-2 in the *par-5(it55)* mutant background, as RNAi of *ftt-2* depletes both FTT proteins and results in sterility (Morton et al., 2002). No mutation in *ftt-2* has been isolated.

Expression of PAR-5 in the Four-Cell Stage *par-5* Mutant Embryos Restores POP-1 Nuclear Asymmetry

The above result suggests that POP-1 nuclear asymmetry is regulated by PAR-5 in early *C. elegans* embryos. To eliminate the possibility that the observed POP-1 defect is a nonspecific consequence of abnormal partition of cytoplasmic factors in *par-5* embryos, we asked whether we could restore POP-1 nuclear asymmetry without restoring the proper early cleavages. *par-5* mutant embryos exhibit observable defects as early as the one-cell stage. We constructed a transgenic strain homozygous for the *par-5(it55)* mutation but carrying a transgene expressing wild-type GFP::PAR-5 under the control of the *med-1* promoter. The *med-1* promoter is not expressed until the four-cell stage (Maduro et al., 2001), by which stage the defect in partition for *par-5(it55)* embryos is already apparent. We scored whether nuclear asymmetry was restored for endogenous POP-1 in 16-cell stage embryos by immunostaining using mabRL2 (Lin et al., 1998). Approximately 69% (n = 32) of *par-5(it55)* 16-cell embryos examined had an equal level of nuclear POP-1 throughout the embryo (Figures 1F–1H). The remaining embryos showed asymmetric levels of nuclear POP-1 between adjacent nuclei. Because *par-5* mutant embryos have abnormal cell divisions, it is difficult to unambiguously identify sister cells in fixed embryos. We scored an embryo as having asymmetric levels of nuclear POP-1 if adjacent nuclei had different levels of POP-1. When GFP::PAR-5 was expressed in the *par-5(it55)* mutant embryos, we observed a decrease in the percentage of embryos with symmetric nuclear POP-1 staining (8%, n = 11). The other 92% showed a clear difference in nuclear POP-1 between adjacent nuclei (Figures 1I–1K). From these results, we conclude that PAR-5 is likely to regulate POP-1 nuclear asymmetry independent of its function in the one-cell stage embryo.

POP-1 and PAR-5 Interact in Wild-Type *C. elegans* Embryos, and This Interaction Depends on the MAP Kinase LIT-1

To test whether PAR-5 regulates POP-1 nuclear asymmetry directly, we examined their physical interaction in *C. elegans* embryo extracts by coimmunoprecipitation (co-IP). When we immunoprecipitated POP-1 using a

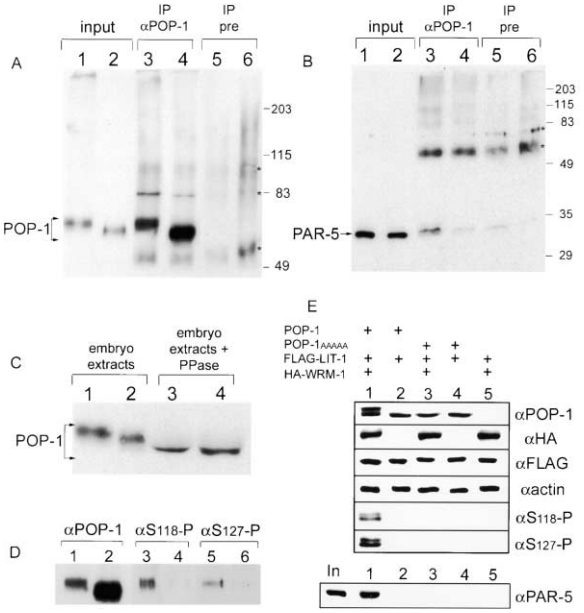

Figure 2. POP-1 and PAR-5 Interact in a LIT-1-Dependent Manner in *C. elegans* Embryos

(A and B) Embryo extracts derived from either wild-type (lanes 3 and 5) or *lit-1(t1512)* (lanes 4 and 6) mutants were immunoprecipitated with either 94I (lanes 3 and 4) or preimmune IgG (lanes 5 and 6), resolved on either a 10% or 15% PAGE, and probed with 94I (A) or PAR-5 antibody (B), respectively. Lanes 1 and 2 correspond to 5% and 0.06% of input extracts in (A) and (B), respectively. Asterisks, nonspecific bands detected by the secondary antibody.

(C) A higher-resolution gel demonstrating that POP-1 is hyperphosphorylated in wild-type (lanes 1 and 3) but hypophosphorylated in *lit-1(t1512)* mutant extracts (lanes 2 and 4). Extracts in lanes 3 and 4 are treated with phosphatases before loading.

(D) Embryo extracts derived from either wild-type (lanes 1, 3, and 5) or *lit-1(t1512)* (lanes 2, 4, and 6) mutants were probed with 94I, anti-S_{118}-P, or anti-S_{127}-P.

(E) Extracts from COS-7 cells expressing POP-1+FLAG-LIT-1+HA-WRM-1 (lane 1), POP-1+FLAG-LIT-1 (lane 2), POP-1_{AAAAA}+FLAG-LIT-1+HA-WRM-1 (lane 3), POP-1_{AAAAA}+FLAG-LIT-1 (lane 4), or FLAG-LIT-1+HA-WRM-1 (lane 5) were probed with the antibodies indicated. After immunoprecipitation with 94I, in vitro-translated PAR-5 was added to perform a pull-down experiment and probed with anti-PAR-5 antibody.

polyclonal antibody, 94I (Lin et al., 1995), we detected coimmunoprecipitated PAR-5 (Figures 2A and 2B). Very little or no PAR-5 was detected when co-IP was performed with the control, preimmune antibody.

Many 14-3-3 binding partners are phosphoproteins, and the phosphorylation regulates the interaction between these partners and 14-3-3 proteins. Therefore, we asked whether interaction between POP-1 and PAR-5 is affected by the phosphorylation state of POP-1. POP-1 is highly phosphorylated in wild-type embryo extracts, as indicated by a reduction of its electrophoretic mobility and a disappearance of these slow-migrating bands upon phosphatase treatment (Figure 2C). This phosphorylation is greatly reduced in extracts isolated from *lit-1(t1512)* mutant or *wrm-1(RNAi)* embryos (Figures 2A and 2C and data not shown), suggesting that LIT-1 activity is at least partially responsible for POP-1 hyperphosphorylation in vivo. While hypophosphorylated POP-1 is immunoprecipitated efficiently with 94I from *lit-1(t1512)*

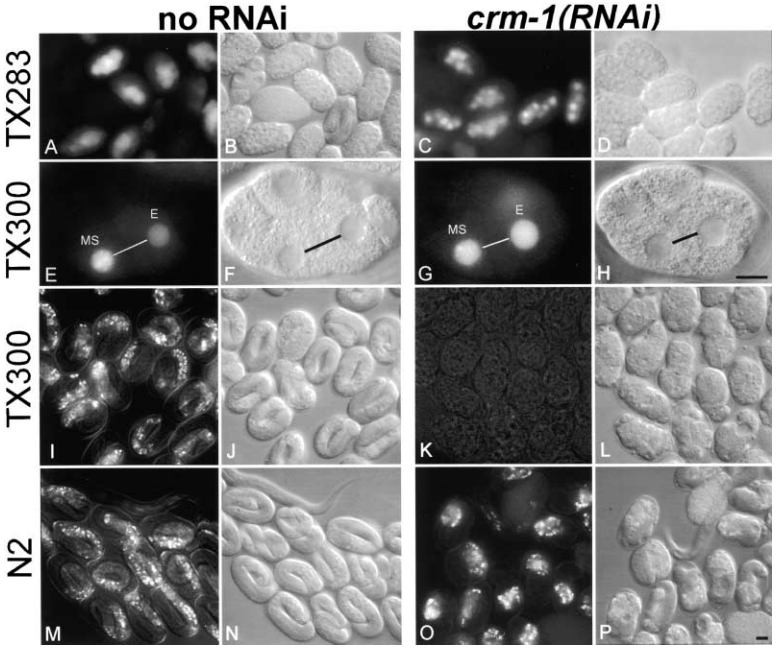

Figure 3. Effect of CRM-1 Depletion on GFP::POP-1 Nuclear Asymmetry and Endoderm Formation

Low (A–D and I–P) and high (E–H) magnification micrographs of non-RNAi or *crm-1(RNAi)* embryos. (A–H) GFP::POP-1 fluorescence (A, C, E, and G) and DIC images (B, D, F, and H) of transgenic embryos harboring $P_{med\text{-}1}$*gfp::pop-1*$_{MutAAA}$ (TX283) or $P_{med\text{-}1}$*gfp::pop-1* (TX300). (I–P) Endoderm differentiation is shown as DIC images (J, L, N, and P) and viewed with polarized microscopy as birefringent granules (I, K, M, and O). MS and E sisters are connected by short lines in (E–H). Scale bar, 10 μm.

embryo extracts, little or no PAR-5 is coimmunoprecipitated (Figures 2A and 2B). Because both POP-1 hyperphosphorylation and its interaction with PAR-5 are dependent on LIT-1 kinase activity, it is likely that LIT-1 phosphorylates POP-1, thereby promoting its interaction with PAR-5 in *C. elegans* embryos.

GFP::POP-1 Nuclear Asymmetry Requires a CRM-1-Dependent Nuclear Export in *C. elegans* Embryos

One of the cellular processes that 14-3-3 proteins have been shown to regulate is nuclear export of their binding partners (Lopez-Girona et al., 1999). Because POP-1 nuclear asymmetry has been suggested to result from differential nucleocytoplasmic redistribution in anterior versus posterior cells, we asked whether nuclear export plays a role in regulating POP-1 nuclear asymmetry. We perturbed nuclear export in the embryo by targeting the *C. elegans* homolog (ZK742.1) of the vertebrate exportin CRM-1 via RNAi. CRM-1 is a highly conserved protein of the karyopherin β superfamily and has been shown to mediate nuclear export of leucine-rich nuclear export sequence (NES)-containing proteins in a variety of organisms (Fornerod et al., 1997; Fukuda et al., 1997; Ossareh-Nazari et al., 1997; Stade et al., 1997).

We first examined whether *crm-1(RNAi)* inhibits nuclear export of POP-1 in *C. elegans* embryos by taking advantage of a transgenic strain expressing predominantly cytoplasmic GFP::POP-1 (TX283, Gay et al., 2003). TX283 expresses mutant POP-1 in which lysines 185, 187, and 188 were mutated to alanine (GFP::POP-1$_{MutAAA}$). Mutation of these three lysines dramatically increases cytoplasmic GFP::POP-1 in all blastomeres without affecting GFP::POP-1 nuclear asymmetry between A-P sister cells (Figures 3A and 3B; Gay et al., 2003). The cytoplasmic accumulation of GFP::POP-1$_{MutAAA}$ was due to a defect in nuclear retention and cannot be rescued by addition of an SV40 nuclear localization sequence (NLS, data not shown). When CRM-1 was depleted by RNAi in TX283, we observed a significant increase in the level of nuclear GFP::POP-1$_{MutAAA}$ (compare Figures 3C and 3A), suggesting that CRM-1 regulates POP-1 nuclear export in *C. elegans* embryos.

We next depleted CRM-1 in the strain TX300 that contains integrated wild-type $P_{med\text{-}1}$*gfp::pop-1* transgenes [Figures 3E–3H; will be referred to as *crm-1(RNAi)*; TX300 hereafter]. Approximately 40% of A-P sisters in the EMS lineage have equal levels of GFP-fluorescence (Figures 3G and 3H). Although the effect on POP-1 nuclear asymmetry in *crm-1(RNAi)*;TX300 embryos is variable, this result suggests that the low level of POP-1 in Wnt/MAPK-responsive cells requires a CRM-1-dependent nuclear export. Consistent with this, addition of an SV40 NLS to GFP::POP-1 did not significantly alter GFP nuclear asymmetry, suggesting that POP-1 nuclear asymmetry is not due to a decreased nuclear import in the posterior cells. The incomplete penetrance of the defect in POP-1 nuclear asymmetry could be a result of incomplete depletion of CRM-1 by RNAi. Alternatively, it could mean that the CRM-1 protein only contributes in part to POP-1 nuclear asymmetry.

The Amino Acids 88–130 Region of POP-1 Is Necessary for its Nuclear Asymmetry

The results above suggest that binding of POP-1 to PAR-5 is regulated by LIT-1-dependent phosphorylation and that this binding facilitates export of POP-1 from the posterior nucleus. To test this model further, we mapped the domain of POP-1 and amino acids essential for its nuclear asymmetry. We generated GFP::POP-1 fusions in which different domains of POP-1 were deleted. Consistent with a previous report, we showed that neither the N-terminal β-catenin binding domain (aa$_{1–43}$) nor the region C-terminal of the HMG domain is required for POP-1 nuclear asymmetry (data not shown; Maduro et al., 2002). Instead, we identified amino acids 88–130 to be necessary for POP-1

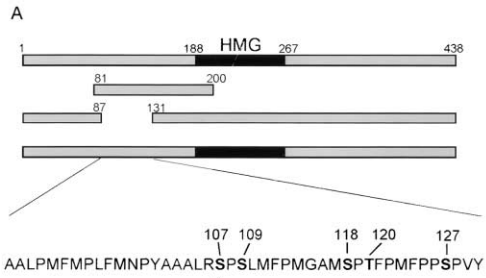

				Nuclear Asymmetry?	rescue the MS defect in *pop-1(zu189)*?	ablate endoderm in wild-type embryos?
				YES	YES (100%, n=31)	NO (0%, n>100)
				NO	NO (0%, n=13)	NO (0%, n>100)
				NO	NO (0%, n=46)	NO (0%, n>100)
A				YES	YES (87%, n=40)	NO (0%, n>100)
	A			YES	YES (94%, n=33)	NO (0%, n>100)
			A	YES	YES (78%, n=9)	NO (0%, n>100)
A	**A**			YES	ND	NO (0%, n>100)
A			**A**	YES	YES (67%, n=6)	NO (0%, n>100)
	A	**A**		YES	YES (94%, n=32)	NO (0%, n>100)
	A	**A**	**A**	VARIABLE*	YES (93%, n=29)	ND
A	**A**		**A**	VARIABLE*	ND	YES (9%, n=23)
A	**A**	**A**	**A**	VARIABLE*	ND	YES (3%, n=30)
A		**A**	**A**	NO	ND	YES (27%, n=11)
	A	**A**	**A**	NO	YES (93%, n=14)	YES (37%, n=8)
A	**A**	**A**	**A**	NO	YES (91%, n=32)	YES (82%, n=22)

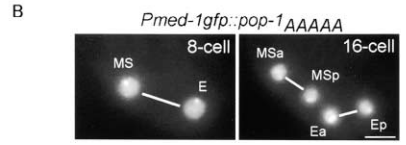

Figure 4. Amino Acids 88–130 of POP-1 Are Required for its Nuclear Asymmetry

(A) Schematic diagram of POP-1 protein and the aa_{88-130} region. The HMG domain (188–267) is shown as a black box. Numbers above the protein indicate positions of amino acids. Portions of POP-1 that have been assayed are shown below. The amino acid sequence of the aa_{88-130} region is shown as single-letter code, and the five potential phosphorylation sites (S_{107}, S_{109}, S_{118}, T_{120}, and S_{127}) are in bold. GFP::POP-1 fusions containing mutations that change these five sites in various combinations to alanines are indicated below the amino acid sequence of aa_{88-130}. The effect on POP-1 nuclear asymmetry as GFP fusions, their ability to rescue the MS defect in the *pop-1(zu189)* mutant embryos, and the effect on endoderm formation in wild-type background are indicated to the right. Asterisks indicate a variable defect and that asymmetry is still detected in some A-P sisters. ND, not determined.

(B) Fluorescence micrographs of eight-cell and 16-cell transgenic embryos harboring $P_{med\text{-}1}$*gfp::pop-1*$_{AAAAA}$. A-P sisters are connected by lines and their names are indicated. Scale bar, 10 μm.

nuclear asymmetry, as embryos carrying the *Pmed-1 gfp::pop-1*$\Delta_{aa88-130}$ transgene exhibit equal levels of nuclear POP-1 between A-P sisters (Figure 4A and data not shown). However, this region is not sufficient for POP-1 nuclear asymmetry, as a GFP fusion protein containing amino acids 81–200 of POP-1 is mostly cytoplasmic with low and equal levels of nuclear POP-1 between A-P sisters (Figure 4A and data not shown).

There are a total of four serines (S_{107}, S_{109}, S_{118}, and S_{127}) and one threonine (T_{120}) within the aa_{88-130} region (Figure 4A). To test whether phosphorylation within this region is important for POP-1 nuclear asymmetry, we changed one or more of these serine/threonine residues to alanine (A) and examined the effect of each mutation on GFP::POP-1 nuclear asymmetry in vivo (Figure 4A). We detected a complete loss of GFP nuclear asymmetry and hence a high level of nuclear GFP in both sisters when all five sites were mutated (100%, $n > 80$; Figure 4). A similar defect was obtained when two combinations of four sites ($S_{107, 118, 127}$ T_{120} or $S_{109, 118, 127}$ T_{120}) were mutated. However, another quadruple mutation (S_{107}A, S_{109}A, S_{118}A, T_{120}A) or two triple mutations (S_{107}A, S_{109}A, S_{127}A and S_{118}A, T_{120}A, S_{127}A) do not abolish GFP nuclear asymmetry (Figure 4A). This result demonstrates that, while none of these five sites alone is essential, serines 107/109, 118, and 127 and threonine 120 are redundantly required for asymmetric nuclear POP-1 levels between A-P sisters in vivo.

GFP::POP-1$_{AAAAA}$ Is Defective Specifically in Nuclear Export but Not Repressor Activity

We also assayed the function of each mutated GFP::POP-1 in vivo. In *pop-1(zu189)* embryos, the endoderm fate is not repressed in the MS blastomere, resulting in both MS and E producing endoderm. The transgenes bearing different mutation combinations were introduced into *pop-1(zu189)* embryos, and their ability to rescue the MS defect, that is, repression of MS-derived endoderm, was assayed. All transgenes containing point mutation(s) examined, including the penta alanine mutation, rescued the MS blastomere defect comparable to a wild-type *gfp::pop-1* transgene (Figure 4A). In rescued embryos, the MS-derived posterior pharynx, characterized by a structure called the grinder, was clearly produced (Figure 5). This result suggests that phosphorylation at any of these five sites is not needed for POP-1 to function as a transcription repressor in the MS blastomere. In addition, in 62% ($n = 32$; data not shown) of *pop-1 (zu189)* and 91% ($n = 22$; Figures 5C–5F) of wild-type embryos expressing GFP::POP-1$_{AAAAA}$, endoderm fate is repressed in the E blastomere as well. The repression of

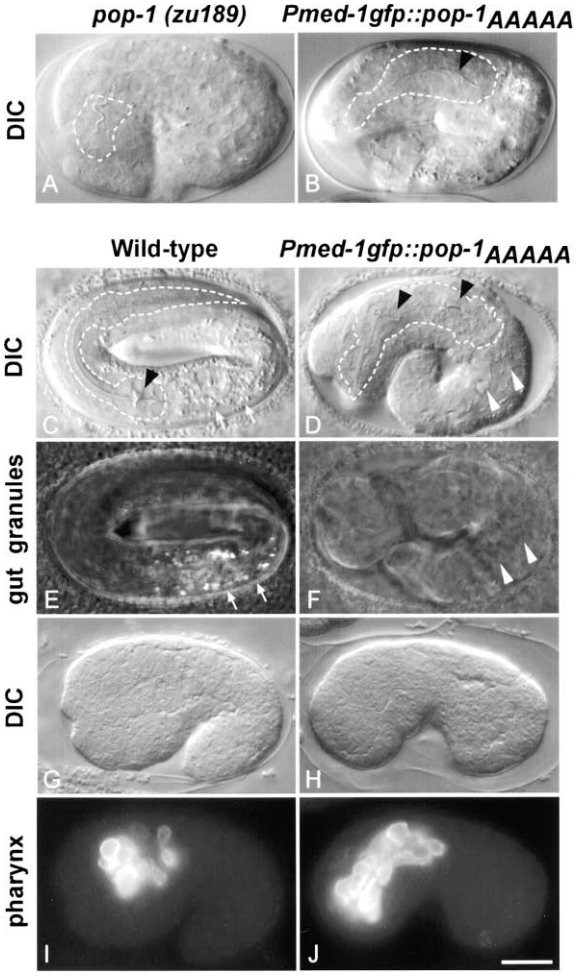

Figure 5. Five Potential Phosphorylation Sites within the Amino Acids 88–130 Region of POP-1 Are Not Required for Its Repressor Activity

Differentiation of intestinal and pharyngeal markers in nontransgenic (left-hand column) and transgenic (right-hand column) embryos carrying $P_{med\text{-}1}$*gfp::pop-1*$_{AAAAA}$. (A and B) *pop-1(zu189)* mutant embryos. (C–J) Wild-type embryos. (C–F) Micrographs of terminally differentiated embryos viewed with DIC (C and D) or polarized light (E and F). The wild-type embryo has a well-differentiated intestine (white arrows), whereas >90% of transgenic embryos have no apparent intestinal cells. White arrowheads in (D) and (F) point to the position where intestine would have been formed in a wild-type embryo. Pharyngeal tissues are outlined in (A)–(D). Black arrowheads point to grinder-like structures characteristic of the posterior pharynx. (G–J) Micrographs of embryos fixed at approximately 450 min after fertilization and stained with 3NB12, a monoclonal antibody to a subset of pharyngeal muscles, and viewed with DIC (G and H) or fluorescence optics (I and J). Scale bar, 10 μm.

endoderm fate in embryos expressing GFP::POP-1$_{AAAAA}$, together with a high level of nuclear POP-1 in the E blastomere, demonstrates that mutations of these potential phosphorylation sites affect specifically POP-1 nuclear export but not its repressor function.

Some wild-type embryos expressing GFP::POP-1$_{AAAAA}$ (23%, n = 22) produce an excess of pharyngeal tissue (Figures 5G–5J), suggesting an E to MS fate transformation. In wild-type embryos, two of the earliest observable differences between the MS and E blastomeres, in addition to different levels of nuclear POP-1, are the division rates and cleavage axes of their daughter cells. The MS daughters divide along the A-P axis 15 min after they are born, whereas the E daughters divide left-right 20–25 min later. In mutants defective in the specification of the E blastomere, including mutants in the Wnt/MAPK signaling pathway, E daughters divide along the A-P axis within 5 min of the MS daughter divisions (Goldstein, 1992; Rocheleau et al., 1997). Similarly, in all embryos expressing GFP::POP-1$_{AAAAA}$ analyzed (n = 7; data not shown), the E daughters divided along the A-P axis within 5 min of MS daughter divisions. These results together demonstrate that expressing GFP::POP-1$_{AAAAA}$ can cause the E blastomere to adopt the fate of its sister blastomere MS.

crm-1(RNAi);TX300 Embryos Fail to Produce Endoderm

A similar defect in endoderm formation was also observed in *crm-1(RNAi)*;TX300 embryos (Figures 3I–3L and data not shown). Every RNAi embryo examined produced no intestinal granules (n > 300) and had an accelerated division rate of E daughters (n = 4). This endoderm repression is dependent on the $P_{med\text{-}1}$*gfp::pop-1* transgene, because 100% of *crm-1(RNAi)* embryos produced gut granules (Figures 3M–3P). Immunofluorescence using the POP-1 antibody confirmed that the nuclear asymmetry of endogenous POP-1 protein is variably affected in *crm-1(RNAi)* embryos similar to GFP::POP-1 in *crm-1(RNAi)*;TX300 embryos. This result strongly suggests that a high level of POP-1 in the E nucleus (rather than an equal level of POP-1 in the nuclei of MS and E) is important for endoderm repression. Consistent with this, we observed a more severe endoderm repression in transgenic animals expressing higher levels of GFP::POP-1$_{AAAAA}$ (data not shown).

LIT-1/WRM-1 Promotes POP-1/PAR-5 Interaction and POP-1 Nuclear Export via Phosphorylation at S_{118} and S_{127} of POP-1

To investigate the mechanism by which these five potential phosphorylation sites regulate POP-1 nuclear asymmetry in vivo, we raised antibodies that recognize phosphorylated POP-1 specifically at either S_{118} (anti-S_{118}-P) or S_{127} (anti-S_{127}-P). The specificity of each antibody to its respective phosphoepitope was confirmed using GFP::POP-1 with either S_{118}A or S_{127}A mutation (data not shown). Both antibodies detect POP-1 protein in wild-type but not *lit-1(t1512)* or *wrm-1(RNAi)* embryo extracts (Figure 2D and data not shown), demonstrating that POP-1 is phosphorylated at S_{118} and S_{127} in *C. elegans* embryos, and phosphorylation of these two sites requires the LIT-1 kinase activity and the β-catenin WRM-1.

POP-1 transgenes carrying mutations that abolish nuclear asymmetry also ablate endoderm, resulting in dead embryos. We had difficulty obtaining sufficient transgenic embryos to perform biochemical analyses. Therefore, we tested whether S_{118} and S_{127} and their phosphorylation were important for POP-1/PAR-5 interaction using transfected mammalian tissue culture cells, COS-7. We detected phosphorylation at S_{118} and S_{127} only when POP-1 was cotransfected into COS-7 cells

Table 1. LIT-1/WRM-1-Stimulated POP-1 Nuclear Export Requires the Five Potential Phosphorylation Sites Essential for POP-1 Asymmetry

Gene Transfected	Subcellular Localization	
	N > C (%)	N ≤ C (%)
pop-1	49.6 ± 2.1	50.4 ± 2.1
pop-1 + *lit-1*	48.5 ± 1.9	51.5 ± 1.9
pop-1 + *lit-1* + *wrm-1*	39.5 ± 1.4	60.5 ± 1.4
pop-1$_{AAAAA}$	49.7 ± 1.8	50.3 ± 1.8
pop-1$_{AAAAA}$ + *lit-1*	49.6 ± 0.7	50.4 ± 0.7
pop-1$_{AAAAA}$ + *lit-1* + *wrm-1*	47.7 ± 1.9	52.3 ± 1.9

WT *pop-1* or *pop-1*$_{AAAAA}$ was transfected into COS-7 cells either in the absence or presence of Flag-*lit-1* and HA-*wrm-1*. Cells were stained with anti-POP-1 monoclonal antibody (Gay et al., 2003), and the POP-1 staining was scored blindly as predominantly nuclear (N > C), equally distributed between nucleus and cytoplasm, or predominantly cytoplasmic (N ≤ C). Results are presented as the average and standard deviation from six sets of experiments. For each experiment, 1000 cells were scored.

with LIT-1 and WRM-1 and not when POP-1 was cotransfected with LIT-1 alone (Figure 2E, lanes 1 and 2). Although we can not rule out an indirect effect, this result strongly suggests that the LIT-1/WRM-1 complex phosphorylates POP-1 at S_{118} and S_{127} in COS-7 cells.

We then tested whether phosphorylation of POP-1 at S_{118} and S_{127} was required for POP-1/PAR-5 interaction. We detected a strong interaction between POP-1 and PAR-5 in a pull-down experiment only when POP-1 was isolated from cells cotransfected with LIT-1 and WRM-1 and was phosphorylated at S_{118} and S_{127} (Figure 2E). Clearly, no PAR-5 was pulled down with POP-1$_{AAAAA}$ (Figure 2E), demonstrating that the LIT-1/WRM-1 complex stimulates POP-1/PAR-5 interaction in vitro via phosphorylation of at least two of these five sites.

Finally, we test whether LIT-1 and WRM-1 stimulate POP-1 nucleocytoplasmic redistribution via these five potential phosphorylation sites. When *pop-1* is transfected into mammalian tissue culture cells, POP-1 protein localizes predominantly in the nucleus in approximately 50% of transfected cells (N > C). In the other 50% of transfected cells, POP-1 distributes either predominantly in the cytoplasm or equally between the cytoplasmic and nuclear compartments (N ≤ C). Upon cotransfection with LIT-1 and WRM-1, POP-1 distribution is changed from N > C to N ≤ C in 10% of transfected cells (Table 1), similar to what was reported previously (Rocheleau et al., 1999). On the contrary, the distribution of POP-1$_{AAAAA}$ is not significantly changed in cells cotransfected with LIT-1 and WRM-1. All together, our results demonstrate that LIT-1 and WRM-1 stimulate POP-1 nucleocytoplasmic redistribution primarily via phosphorylation of at least two of these five sites.

Nuclear GFP::LIT-1 Exhibits an Asymmetric Pattern between A-P Sisters Reciprocal to that of Nuclear GFP::POP-1

If phosphorylation of POP-1 by LIT-1 promotes POP-1 association with PAR-5 and subsequent nuclear export in the posterior Wnt/MAPK-responsive blastomere, POP-1 must be differentially phosphorylated by LIT-1 between the nuclei of A-P sisters. We could not prove this hypothesis directly, because anti-S_{118}-P and

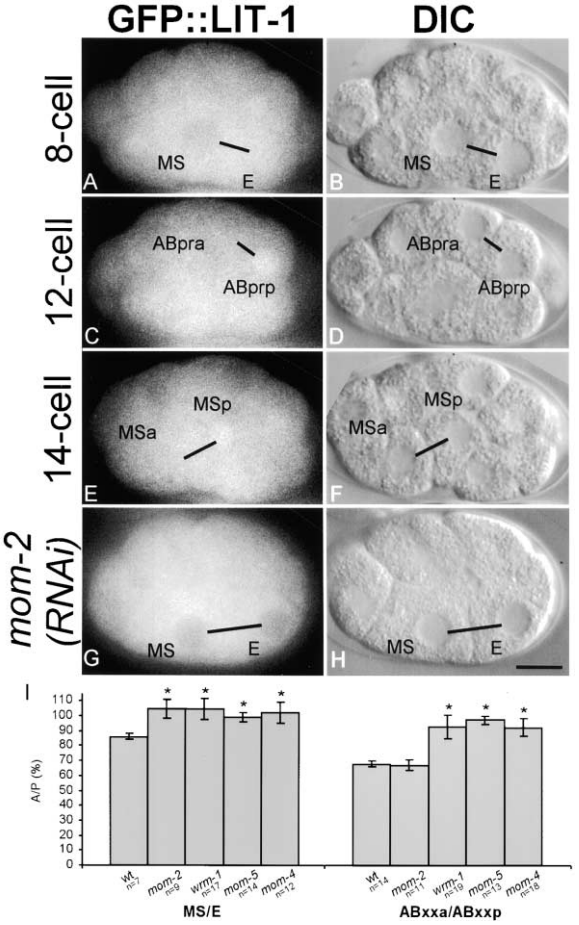

Figure 6. GFP::LIT-1 Nuclear Asymmetry between A-P Sisters Is Reciprocal to GFP::POP-1 Nuclear Asymmetry

Micrographs showing GFP::LIT-1 fluorescence (A, C, E, and G) and DIC images (B, D, F, and H) in wild-type or *mom-2(RNAi)* backgrounds. (A, B, G, and H) eight-cell, (C and D) 12-cell, (E and F) 14-cell. Images are selected from movie recordings. The black line in each panel connects a pair of A-P sister nuclei whose names are indicated and which are equally focused at that particular focal plane. (I) Relative levels (A/P%) of nuclear GFP::LIT-1 between MS and E (left-hand graphs) and ABxxa and ABxxp (right-hand graphs) in wild-type, *mom-2(RNAi)*, *wrm-1(RNAi)*, *mom-5(RNAi)*, and *mom-4 (RNAi)* embryos. *p < 0.001. Scale bar, 10 μm.

anti-S_{127}-P detect primarily a non-POP-1 nuclear protein in the immunofluorescence assay (data not shown). However, we detected an elevated level of nuclear GFP::LIT-1 in the posterior cells compared to their anterior sisters (Figure 6, see also next paragraph), a pattern reciprocal to that of POP-1, supporting the hypothesis that POP-1 is differentially phosphorylated by LIT-1 between the nuclei of A-P sisters.

The GFP::LIT-1 was detected, both cytoplasmic and nuclear, in every blastomere. The nuclear GFP::LIT-1, despite a low level, was detected in a dynamic pattern both temporally and spatially. GFP::LIT-1 was consistently enriched in the interphase nuclei of only a subset of early blastomeres. Comparison with the corresponding DIC images revealed that, at the eight-cell stage, nuclear GFP::LIT-1 was enriched in the interphase E blastomere but not in the MS blastomere (Figures 6A,

6B, and 6I). At the 12-cell stage, interphase nuclear GFP::LIT-1 was enriched in four of the great granddaughters of the AB blastomere (ABarp, ABalp, ABprp, and ABplp, all posterior daughters of A-P divisions) but not their anterior sister cells (Figures 6C, 6D, and 6I and data not shown). Nuclear enrichment was also observed at the 14-cell stage in the posterior daughters of MS and E, MSp and Ep, respectively, but not their anterior daughters (Figures 6E and 6F and data not shown). After the 14-cell stage, the GFP signal was too low for us to continue evaluating. This result strongly supports the model that elevated POP-1 nuclear export in the posterior daughter cells of A-P divisions is a result of a higher level of LIT-1 kinase in the posterior nuclei.

If POP-1 nuclear asymmetry is regulated through phosphorylation by LIT-1, whose own nuclear level is reciprocally asymmetric between A-P sisters, the question then becomes what regulates the asymmetry of LIT-1. We have examined the effect on GFP::LIT-1 in embryos depleted of some components of the Wnt/MAPK signaling pathway, *mom-2*, *mom-5*, *wrm-1*, or *mom-4*. We observed that depletion of any of these four genes resulted in a loss of the enrichment for interphase nuclear GFP::LIT-1 in E (88%, n = 16; 93%, n = 15; 100%, n = 19; and 100%, n = 28, respectively) (Figures 6G, 6H, and 6I and data not shown), suggesting that the level of nuclear LIT-1 in E is regulated by both Wnt and MAPK signaling pathways. The enrichment for interphase nuclear GFP::LIT-1 in ABxxp was also abolished when *mom-5* (93%, n = 15), *wrm-1* (100%, n = 19), or *mom-4* (100%, n = 28) was depleted (Figure 6I and data not shown). However, the enrichment in ABxxp was still observed in *mom-2(RNAi)* embryos (100%, n = 16; Figure 6I and data not shown), suggesting that while some components in the Wnt and MAPK signaling pathways are involved in regulating the level of nuclear LIT-1 in ABxxp, the MOM-2 Wnt signaling molecule is not required. Taken together, these results demonstrate that the upstream components of the Wnt/MAPK pathway regulate POP-1 nuclear asymmetry in part by regulating the level of nuclear LIT-1 in posterior cells.

Discussion

We show here that Wnt/MAPK signaling regulates POP-1 nuclear asymmetry in early embryos by regulating its interaction with PAR-5. First, POP-1 nuclear asymmetry is disrupted in *par-5* mutant embryos. Reintroduction of PAR-5 into four-cell staged *par-5* mutant embryos restores POP-1 nuclear asymmetry. Second, POP-1 is hyperphosphorylated and interacts with PAR-5 in embryo extracts. Both POP-1 hyperphosphorylation and its interaction with PAR-5 depend on the LIT-1 kinase. Third, we identify five potential POP-1 phosphorylation sites that are required for its nuclear asymmetry and for PAR-5 interaction following stimulation by the LIT-1/WRM-1 complex in vitro. At least two of these five amino acids are phosphorylated in vivo. Our data support the model that PAR-5 regulates POP-1 nuclear asymmetry by facilitating its nuclear export, as inhibition of nuclear export also leads to a loss of POP-1 nuclear asymmetry. In addition, we show that a GFP::LIT-1 reporter also exhibits nuclear asymmetry between A-P sisters but in a reciprocal pattern to that of POP-1 and that the GFP::LIT-1 nuclear asymmetry requires regulation by the upstream kinase as well as Wnt signaling.

It is clear that a Wnt-independent mechanism regulates the steady-state level of nuclear POP-1 in every embryonic cell. This is supported by two observations. (1) In the absence of input from Wnt/MAPK signaling (either in signaling mutants or in transgenic animals expressing GFP::POP-1_{AAAAA}), POP-1 remains nuclear in every cell. (2) Mutations of lysines 185, 187, and 188 to alanines result in a defect in nuclear retention of POP-1 in every cell but do not affect A-P asymmetry (Gay et al., 2003). What our results present is a Wnt/MAPK-dependent mechanism that facilitates nuclear export of POP-1 preferentially in the signal-responsive cell, resulting in the observed A-P nuclear asymmetry (Figure 7). Our data demonstrate that Wnt/MAPK signaling results in a higher level of nuclear LIT-1 kinase in the posterior cell. The LIT-1/WRM-1 complex promotes POP-1/PAR-5 interaction via phosphorylation of POP-1 at two and perhaps more of five identified potential phosphorylation sites.

The mechanism by which PAR-5 results in a low level of nuclear POP-1 remains unclear, although a role for the exportin CRM-1 is suggested. We have shown previously that acetylation of POP-1 by CBP-1 at K_{185} (and likely K_{187} and K_{188}) facilitates POP-1 nuclear retention (Gay et al., 2003). Therefore, PAR-5 could result in a low level of nuclear POP-1 by antagonizing the effect of acetylation at these three lysines, by sequestering POP-1 in the cytoplasm, or by promoting POP-1 nuclear export. 14-3-3 proteins have been shown to promote nuclear export through different mechanisms. These include interfering with the NLS of the target protein, allowing recognition or binding by the CRM-1-dependent nuclear export machinery, and providing an NES located at their own C termini (Lopez-Girona et al., 1999). Despite our efforts, we have not yet identified an NES of POP-1 that functions in its export in *C. elegans* embryos (unpublished data). Because of their roles in POP-1 nuclear retention, acetylated lysines 185, 187, and 188 could interact with nuclear export machinery and complicate the identification of an NES in vivo. Further analyses are underway to elucidate the mechanism by which PAR-5 binding facilitates POP-1 nuclear export.

The majority of 14-3-3 proteins form dimers and interact with their targets via cooperative binding to two phosphorylated residues on their target proteins (see review by Tzivion and Avruch, 2002). None of the five potential phosphorylation sites important for POP-1 nuclear asymmetry is a perfect match to known 14-3-3 binding sites. The precise role of each of the potential phosphorylation sites in POP-1 nuclear asymmetry in vivo awaits further investigation.

What Is the First Asymmetry?

POP-1 nuclear asymmetry is observed between all sisters derived from A-P divisions throughout early embryogenesis (Lin et al., 1998). LIT-1 appears to function in regulating POP-1 nuclear asymmetry throughout all lineages examined (Rocheleau et al., 1999; unpublished data). We now show that WRM-1 and MOM-4 regulate nuclear LIT-1 levels in the posterior cells, which alone

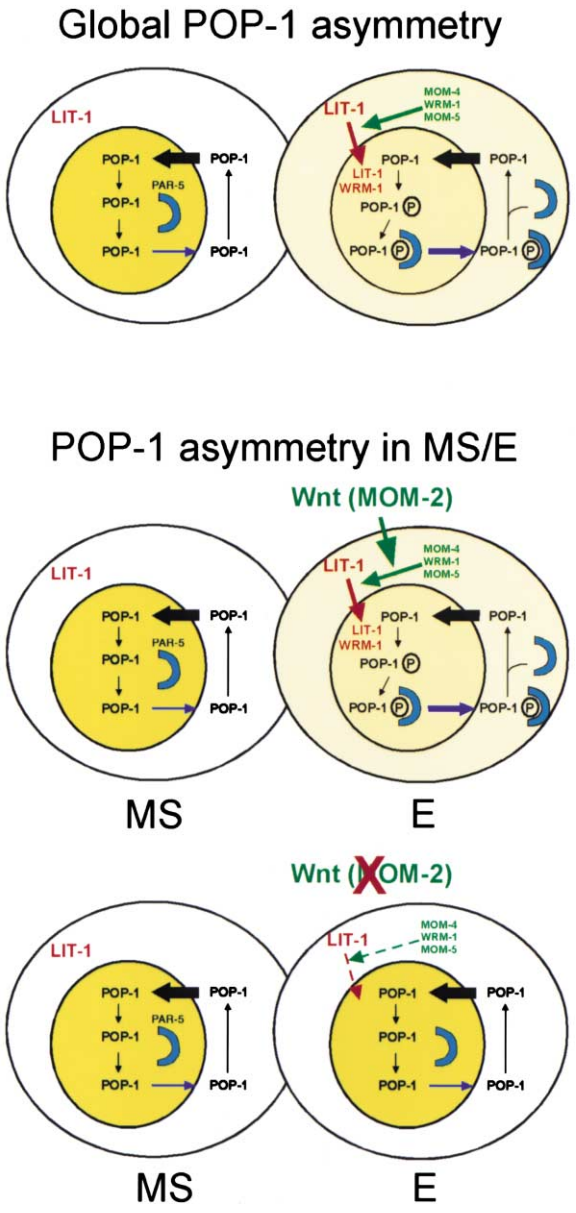

Figure 7. Model

We propose that POP-1 nuclear asymmetry throughout the early *C. elegans* embryo is a result of a PAR-5-mediated nuclear export that occurs predominantly in the posterior cells. In this model, the upstream Wnt/MAP kinase components result in a high nuclear LIT-1 in posterior nuclei. A higher level of nuclear LIT-1, in combination with the presence of the WRM-1 protein, results in hyperphosphorylation of POP-1 in the posterior nuclei. Phosphorylation of POP-1 by LIT-1 creates a binding site(s) for PAR-5 (blue crescent). Binding to PAR-5 facilitates the nuclear export of POP-1, resulting in an observed lower level of nuclear POP-1 in posterior cells. In the E blastomere, input from Wnt signaling (MOM-2) is also required for a high level of nuclear LIT-1. The level of POP-1 is indicated by different shades of yellow, with the brightest yellow representing the highest level.

could account for how these genes regulate POP-1 nuclear asymmetry. However, it is unlikely that WRM-1 and MOM-4 regulate POP-1 nuclear asymmetry solely by regulating the level of LIT-1 in the posterior nuclei, because WRM-1 is essential for and MOM-4 enhances LIT-1 kinase activity in vitro, suggesting multiple levels of regulation.

The signal leading to POP-1 nuclear asymmetry in blastomeres other than MS and E has not been identified. It appears that neither the P2 blastomere nor MOM-2 is required (Lin et al., 1998; unpublished data). Anterior-posterior polarity in *C. elegans* embryos is established upon fertilization and is propagated through the subsequent divisions. A key challenge is to identify the first cue that establishes A-P differences recognized by the Wnt/MAPK signaling pathway and to understand how this cue is propagated through subsequent divisions. In most eukaryotes, cells in a tissue exhibit a common polarity within the plane of the tissue, a phenomenon known as planar cell polarity (see review by Adler and Lee, 2001). Many key members functioning in regulating the planar cell polarity have been identified in other organisms, including Frizzled and Nemo, which are homologs of MOM-5 and LIT-1, respectively (Choi and Benzer, 1994; Adler and Lee, 2001). This suggests the intriguing possibility that global POP-1 A-P polarity in *C. elegans* embryos may be regulated by a mechanism similar to that regulating planar cell polarity.

The level of nuclear LIT-1 (as well as nuclear POP-1) in E requires additional input from P2 via Wnt signaling (Rocheleau et al., 1997; Thorpe et al., 1997; Lin et al., 1998; and this work). It is not clear why Wnt signaling is needed for the E blastomere or how it achieves this regulation. One possible convergent point for Wnt and MAPK pathways is the WRM-1 protein, which (1) is an integral part of LIT-1 kinase activity, (2) is required for the enrichment of nuclear LIT-1 in the posterior cells, and (3) shares similarity to the known Wnt component, β-catenin. Perhaps Wnt signaling activates WRM-1, which otherwise is inactive in E, promoting a high level of nuclear LIT-1.

Is POP-1 Quantitatively and Qualitatively Different between Anterior and Posterior Nuclei?

The difference in the levels of nuclear POP-1 between A-P sisters, assayed either by antibody staining or by GFP fluorescence, appears no more than perhaps five folds. It is intriguing, then, how such a small difference in POP-1 level results in a developmental switch of anterior cell fate. A particularly interesting question arises: is it the absolute abundance of POP-1 in the anterior nucleus or the relative abundance of POP-1 between A-P sisters that is important for the cell fate difference? That is, would an increase in POP-1 levels in E be sufficient to transform the E fate to an MS fate? Because one can overexpress GFP::POP-1 from transgenes in wild-type embryos without disturbing embryogenesis (Maduro et al., 2002), this would suggest that perhaps the absolute abundance of POP-1 is not critical as long as the asymmetry is maintained between A-P sisters. However, we observed a GFP::POP-1-dependent endoderm repression in *crm-1(RNAi)* embryos. Endogenous POP-1 levels are equal between MS and E in some *crm-1(RNAi)* embryos, and yet all embryos produce intestine. However, no *crm-1(RNAi)* embryos that express GFP::POP-1 produce intestine. Although we can not rule out the possibility that overexpression of POP-1 exacerbates the defect

in nuclear export by saturating the nuclear export machinery, we prefer the explanation that a high level of POP-1 in E, rather than an equal level of POP-1 between MS and E, is needed to repress endoderm. Furthermore, although GFP::POP-1_{AAAAA} is detected equally between nuclei of MS and E, it represses MS-derived endoderm in 91% of *pop-1(zu189)* embryos and E-derived endoderm in only 62% of *pop-1(zu189)* embryos. This suggests that POP-1 is qualitatively different in MS and E and that a higher level of POP-1 is needed to repress endoderm in the E blastomere than in the MS blastomere.

This qualitative difference could be due to the differential presence of a POP-1-interacting protein, the differential modification of nuclear POP-1 in MS and E, or both. It has been shown that the mammalian LIT-1 homolog NLK phosphorylates TCF-4 at two distinct amino acids (T_{178} and T_{189}), which inhibits the DNA binding activity of the β-catenin/TCF complex in vitro (Ishitani et al., 2003). Therefore, it is possible that phosphorylation of POP-1 by LIT-1, in addition to promoting its association with PAR-5, changes its affinity toward target DNA sequences or other factors in the E nucleus. However, we currently have no evidence that LIT-1 also regulates POP-1 DNA binding activity on the corresponding two sites (S_{71} and S_{82}), as mutation of these two sites to alanines does not result in any detectable defect with respect to nuclear asymmetry or function in embryos (unpublished data).

Nuclear Export of TCF/LEF Transcription Factors: A Conserved Mechanism?

Is the Wnt/MAPK-induced nuclear export of a TCF protein described here a *C. elegans*-specific phenomenon? *C. elegans* POP-1 is the only TCF protein known to undergo nucleocytoplasmic redistribution upon Wnt signaling. TCF/LEF proteins appear to be constitutive nuclear proteins in all other organisms examined so far. In addition, the canonical Wnt signaling pathway results in the activation of Wnt-responsive genes via a TCF/β-catenin complex. It would seem counterintuitive to lower the level of nuclear TCF/LEF proteins in order to activate transcription in this model. Therefore, it is possible that the Wnt-induced nuclear export of TCF proteins only occurs in *C. elegans* embryos where POP-1 functions mainly as a repressor. However, two results suggest that Wnt signaling-induced nuclear export of TCF proteins may not be limited to *C. elegans* embryos. First, it has been shown in flies that reduction of dTcf partially suppresses, whereas its overexpression enhances, the *wingless* mutant phenotype (Cavallo et al., 1998). This is consistent with a model where Wnt signaling lowers the level of TCF proteins. Second, in the development of *C. elegans* male tail, Wnt signaling lowers the nuclear level of POP-1 in the cell T.p, whose fate is specified by POP-1 (Herman, 2001). LIT-1 homologs have been shown to regulate the activity of TCF/LEF proteins in a variety of organisms (Choi and Benzer, 1994; Hyodo-Miura et al., 2002; Ishitani et al., 2003), and 14-3-3 proteins are highly conserved among eukaryotes. Therefore, it is an intriguing possibility that LIT-1 homologs and 14-3-3 proteins may also regulate nuclear export of TCF/LEF in other organisms.

Experimental Procedures

Strains

N2 was used as the wild-type strain. Genetic markers used in this study are LGI, *pop-1(zu189)*, *dpy-5(e61)*; LGIII, *unc-119(ed3)*, *lit-1 (t1512)*, *unc32(e189)*; and LGIV, *par-5(it55)*, *unc-22(e66), dnT1(IV;V)*. The following transgenes are maintained as extrachromosomal arrays in respective strains: $P_{med\text{-}1}$*SV40 NLS::gfp::pop-1* (pRL768) in TX350(*teEx70*); $P_{med\text{-}1}$*gfp::pop-1* (pRL769) in TX352(*teEx72*); $P_{med\text{-}1}$*gfp::pop-1*$_{mutAAA}$ (pRL626) in TX283(*teEx26*); $P_{med\text{-}1}$*SV40NLS::gfp::pop-1*$_{mutAAA}$ (pRL777) in TX438(*teEx115*); $P_{med\text{-}1}$*gfp::par-5* (pRL779) in TX385(*teEx95*). TX324(*teEx48*) and TX326(*teEx50*) were generated by microparticle bombardment (Praitis et al., 2001) of the plasmid $P_{pie\text{-}1}$*gfp::lit-1* (pRL710) and show identical GFP::LIT-1 patterns. The *par-5(it55)unc-22(e66)/dnT1;teEx95* strain (TX374) was generated by crossing TX385 males with KK299 [*par-5(it55)unc22(e66)*(IV)/*dnT1*(IV;V), a gift from Ken Kemphues] hermaphrodites, backcrossing the F1 non-Unc males to KK299 and picking F2 Unc hermaphrodites segregating *unc-22*, *dnT1*, and GFP. TX300 (*teIs3*$P_{med\text{-}1}$*gfp::pop-1*) was derived from integrating the transgene in JR2308 (a gift from Joel Rothman and Morris Maduro) after EMS mutagenesis and screening for F2 segregating 100% non-Unc progeny.

Plasmid Construction

Most GFP fusions were constructed using gateway cloning technology (Invitrogen). Destination vectors containing $P_{med\text{-}1}$*SV40NLS::gfp* (pRL706) and $P_{med\text{-}1}$*gfp* (pRL707) sequences were generated by replacing the BamHI-NcoI *gfp::pop-1* fragment of pMM414 (Maduro et al., 2002) with *NLS::gfp* (from the Fire vector kit pPD104.53) and *gfp*, respectively, and then blunt-end ligating the Gateway cassette (reading frame A) via an EcoRV site downstream of the *gfp* sequence. The GFP::LIT-1-expressing plasmid was generated by introducing *lit-1* coding sequence into the $P_{pie\text{-}1}$*gfp* destination vector pID3.01B (a gift from Geraldine Seydoux). All site-directed mutageneses were performed using the QuikChange Site-Directed Mutagenesis kit (Stratagene).

Analysis of Embryos and Imaging

Embryos of the *unc-22* animals segregated from KK299 and TX374 were processed for POP-1 immunostaining as described previously (Lin et al., 1998). Imaging of immunofluorescence and live embryos was performed using an Axioplan microscope equipped with epifluorescence, polarizing, and differential interference contrast (DIC) optics and a MicroMax-512EBFT CCD camera as described previously (Rogers et al., 2002). Intestinal cells were identified by their birefringent gut-specific granules under polarized optics. At each time point of live imaging, GFP fluorescence and DIC images were collected from a selected focal plane to follow particular anterior-posterior sister pairs. All live images were collected as 16-bit with the raw pixel values within the linear range of the CCD camera and scaled to 8-bit using the custom program EditView4D (Rogers et al., 2002). Quantification of GFP::LIT-1 was performed using the ImageJ program and analyzed using the Student's t test for the statistical significance.

RNA Interference

The dsRNA for *crm-1(ZK742.1)*, *mom-2, mom-4*, and *mom-5* were synthesized from corresponding cDNA or genomic DNA, and RNAi was performed by injection (Rogers et al., 2002). *wrm-1(RNAi)* was performed by feeding L3 larvae to adulthood (Timmons and Fire, 1998). Embryos laid from 16 to 30 hr after injection or 24 to 30 hr after feeding were collected and either allowed to differentiate for 8 more hr, a period long enough for wild-type control embryos to hatch, or processed for imaging. *crm-1(RNAi)* animals have ~90% reduction of *crm-1* mRNA (data not shown) and produce 50% ($n > 200$) dead embryos. RNAi with the other genes resulted in 100% dead embryos in our hands. We observed a decrease in the overall level of GFP::LIT-1 in the *mom-4(RNAi)* embryos ($n > 100$), suggesting that MOM-4 might also be required for LIT-1 stability.

Antibody Production and Biochemical Analyses

Anti-S_{118}-P and anti-S_{127}-P antibodies were generated by immunizing rabbits with peptides phosphorylated at respective residues. The

antibodies were precleared with nonphosphorylated peptide and then affinity purified using phosphorylated peptides (Bethyl Laboratory, Inc.). The affinity-purified antibodies react with corresponding phosphorylated (compared to the unphosphorylated) peptides with a >1000-fold higher affinity by ELISA assays.

Embryos were collected from gravid adults and sonicated in the co-IP buffer to yield extracts (Calvo et al., 2001). *lit-1(t1512)* mutant animals were shifted to 25°C at L3 prior to the embryo collection. For each co-IP reaction, 400 μg of extracts were incubated overnight at 4°C with protein A beads coated with either affinity-purified 94I (Lin et al., 1995) or preimmune IgG. The beads were washed three times in the co-IP buffer with 500 mM KCl and twice in the co-IP buffer. The immunoprecipitates were subjected to Western blotting analyses using either anti-PAR-5 antibody (a gift from Andy Golden and Diane Shakes) or 94I and visualized using an ECL system (Amersham). For the gel shown in Figure 2C, 20 μg of embryo extracts were incubated with 20 U of calf intestinal alkaline phosphatase (Roche) at 37°C for 1.5 hr prior to SDS-PAGE.

Transfection was performed using the COS-7 cells. For each co-transfection, 2 μg of CMX plasmid-encoding POP-1, 9 μg each of pcDNA3-Flag-LIT-1, pcDNA3-HA-WRM-1 (provided by Craig Mello; Rocheleau et al., 1999), or appropriate empty vectors were used. After 48 hr, cells were collected and subjected to three cycles of freezing and thawing in co-IP buffer to yield extracts (Calvo et al., 2001). Extracts were either used to perform Western blot analyses with various antibodies or co-IP using 94I-coupled protein G beads as described above (Calvo et al., 2001). After co-IP, 10% of beads were subjected to Western analyses, whereas 90% were incubated with PAR-5 proteins (50 mM Tris [pH 8.0]; 100 mM NaCl; 0.02% Tween 20; 0.05% BSA) translated in rabbit reticulocyte lysates (Promega) for a pull-down assay (Gay et al., 2002). After 6 hr at 4°C, the protein G beads were pelleted, washed five times (50 mM Tris [pH 8.0]; 150 mM NaCl; 0.02% Tween 20; and proteases inhibitors), and subjected to Western blotting with the anti-PAR-5 antibody. Antibody dilutions were 94I (1:500), anti-PAR-5 (rabbit, 1:2000), anti-S_{118}-P (1:1000), anti-S_{127}-P (1:1000), anti-Flag (mouse, 1:2000, Sigma), anti-HA (mouse, 1:2000, Covance-Babco), and anti-actin (mouse, 1:200,000, Chemicon International).

Acknowledgments

The authors would like to thank Drs. Scott Robertson, Keith Wharton, and Eric Olson for their comments on the manuscript; Melanie Reuben and Dominica Calvo for technical assistance; and Morris Maduro, Joel Rothman, Andy Golden, Diane Shakes, Geraldine Seydoux, Ken Kemphues, Craig Mello, and Andy Fire for various reagents. M-C.L., R.O., and R.L. are supported by the NIH grant (HD37933) (to R.L.). R.L. is also supported by a grant from March of Dimes (FY01-265). F.G. and Y.S. are supported by the grant GM58012 to Y.S.

Received: September 4, 2003
Revised: February 10, 2004
Accepted: February 10, 2004
Published: April 1, 2004

References

Adler, P.N., and Lee, H. (2001). Frizzled signaling and cell-cell interactions in planar polarity. Curr. Opin. Cell Biol. *13*, 635–640.

Bullions, L.C., and Levine, A.J. (1998). The role of beta-catenin in cell adhesion, signal transduction, and cancer. Curr. Opin. Oncol. *10*, 81–87.

Calvo, D., Victor, M., Gay, F., Sui, G., Luke, M.P., Dufourcq, P., Wen, G., Maduro, M., Rothman, J., and Shi, Y. (2001). A POP-1 repressor complex restricts inappropriate cell type-specific gene transcription during *Caenorhabditis elegans* embryogenesis. EMBO J. *20*, 7197–7208.

Cavallo, R.A., Cox, R.T., Moline, M.M., Roose, J., Polevoy, G.A., Clevers, H., Peifer, M., and Bejsovec, A. (1998). *Drosophila* Tcf and Groucho interact to repress Wingless signalling activity. Nature *395*, 604–608.

Choi, K.W., and Benzer, S. (1994). Rotation of photoreceptor clusters in the developing *Drosophila* eye requires the *nemo* gene. Cell *78*, 125–136.

Fornerod, M., Ohno, M., Yoshida, M., and Mattaj, I.W. (1997). CRM1 is an export receptor for leucine-rich nuclear export signals. Cell *90*, 1051–1060.

Fu, H., Subramanian, R.R., and Masters, S.C. (2000). 14-3-3 proteins: structure, function, and regulation. Annu. Rev. Pharmacol. Toxicol. *40*, 617–647.

Fukuda, M., Asano, S., Nakamura, T., Adachi, M., Yoshida, M., Yanagida, M., and Nishida, E. (1997). CRM1 is responsible for intracellular transport mediated by the nuclear export signal. Nature *390*, 308–311.

Gay, F., Barath, P., Desbois-Le Péron, C., Métivier, R., Le Guével, R., Birse, D., and Salbert, G. (2002). Multiple phosphorylation events control chicken ovalbumin upstream promoter transcription factor I orphan nuclear receptor activity. Mol. Endocrinol. *16*, 1332–1351.

Gay, F., Calvo, D., Lo, M.-C., Ceron, J., Maduro, M., Lin, R., and Shi, Y. (2003). Acetylation regulates subcellular localization of the Wnt signaling nuclear effector POP-1. Genes Dev. *17*, 717–722.

Goldstein, B. (1992). Induction of gut in *Caenorhabditis elegans* embryos. Nature *357*, 255–257.

Herman, M. (2001). *C. elegans* POP-1/TCF functions in a canonical Wnt pathway that controls cell migration and in a noncanonical Wnt pathway that controls cell polarity. Development *128*, 581–590.

Hermann, G.J., Leung, B., and Priess, J.R. (2000). Left-right asymmetry in *C. elegans* intestine organogenesis involves a LIN-12/Notch signaling pathway. Development *127*, 3429–3440.

Hyodo-Miura, J., Urushiyama, S., Nagai, S., Nishita, M., Ueno, N., and Shibuya, H. (2002). Involvement of NLK and Sox11 in neural induction in *Xenopus* development. Genes Cells *7*, 487–496.

Ishitani, T., Ninomiya-Tsuji, J., Nagai, S., Nishita, M., Meneghini, M., Barker, N., Waterman, M., Bowerman, B., Clevers, H., Shibuya, H., and Matsumoto, K. (1999). The TAK1-NLK-MAPK-related pathway antagonizes signalling between beta-catenin and transcription factor TCF. Nature *399*, 798–802.

Ishitani, T., Ninomiya-Tsuji, J., and Matsumoto, K. (2003). Regulation of lymphoid enhancer factor 1/T-cell factor by mitogen-activated protein kinase-related Nemo-like kinase-dependent phosphorylation in Wnt/beta-catenin signaling. Mol. Cell. Biol. *23*, 1379–1389.

Kaletta, T., Schnabel, H., and Schnabel, R. (1997). Binary specification of the embryonic lineage in *Caenorhabditis elegans*. Nature *390*, 294–298.

Lin, R., Thompson, S., and Priess, J.R. (1995). *pop-1* encodes an HMG box protein required for the specification of a mesoderm precursor in early *C. elegans* embryos. Cell *83*, 599–609.

Lin, R., Hill, R.J., and Priess, J.R. (1998). POP-1 and anterior-posterior fate decisions in *C. elegans* embryos. Cell *92*, 229–239.

Lopez-Girona, A., Furnari, B., Mondesert, O., and Russell, P. (1999). Nuclear localization of Cdc25 is regulated by DNA damage and a 14-3-3 protein. Nature *397*, 172–175.

Maduro, M.F., Meneghini, M.D., Bowerman, B., Broitman-Maduro, G., and Rothman, J.H. (2001). Restriction of mesendoderm to a single blastomere by the combined action of SKN-1 and a GSK-3beta homolog is mediated by MED-1 and -2 in *C. elegans*. Mol. Cell *7*, 475–485.

Maduro, M.F., Lin, R., and Rothman, J.H. (2002). Dynamics of a developmental switch: recursive intracellular and intranuclear redistribution of *Caenorhabditis elegans* POP-1 parallels Wnt-inhibited transcriptional repression. Dev. Biol. *248*, 128–142.

Meneghini, M.D., Ishitani, T., Carter, J.C., Hisamoto, N., Ninomiya-Tsuji, J., Thorpe, C.J., Hamill, D.R., Matsumoto, K., and Bowerman, B. (1999). MAP kinase and Wnt pathways converge to downregulate an HMG-domain repressor in *Caenorhabditis elegans*. Nature *399*, 793–797.

Morton, D.G., Shakes, D.C., Nugent, S., Dichoso, D., Wang, W., Golden, A., and Kemphues, K.J. (2002). The *Caenorhabditis elegans par-5* gene encodes a 14-3-3 protein required for cellular asymmetry in the early embryo. Dev. Biol. *241*, 47–58.

Ossareh-Nazari, B., Bachelerie, F., and Dargemont, C. (1997). Evidence for a role of CRM1 in signal-mediated nuclear protein export. Science *278*, 141–144.

Pandur, P., and Kuhl, M. (2001). An arrow for wingless to take-off. Bioessays *23*, 207–210.

Polakis, P. (2000). Wnt signaling and cancer. Genes Dev. *14*, 1837–1851.

Praitis, V., Casey, E., Collar, D., and Austin, J. (2001). Creation of low-copy integrated transgenic lines in *Caenorhabditis elegans*. Genetics *157*, 1217–1226.

Rocheleau, C.E., Downs, W.D., Lin, R., Wittmann, C., Bei, Y., Cha, Y.H., Ali, M., Priess, J.R., and Mello, C.C. (1997). Wnt signaling and an APC-related gene specify endoderm in early *C. elegans* embryos. Cell *90*, 707–716.

Rocheleau, C.E., Yasuda, J., Shin, T.H., Lin, R., Sawa, H., Okano, H., Priess, J.R., Davis, R.J., and Mello, C.C. (1999). WRM-1 activates the LIT-1 protein kinase to transduce anterior/posterior polarity signals in *C. elegans*. Cell *97*, 717–726.

Rogers, E., Bishop, J.D., Waddle, J.A., Schumacher, J.M., and Lin, R. (2002). The aurora kinase AIR-2 functions in the release of chromosome cohesion in *Caenorhabditis elegans* meiosis. J. Cell Biol. *157*, 219–229.

Schroeder, D.F., and McGhee, J.D. (1998). Anterior-posterior patterning within the *Caenorhabditis elegans* endoderm. Development *125*, 4877–4887.

Shin, T.H., Yasuda, J., Rocheleau, C.E., Lin, R., Soto, M., Bei, Y., Davis, R.J., and Mello, C.C. (1999). MOM-4, a MAP kinase kinase kinase-related protein, activates WRM-1/LIT- 1 kinase to transduce anterior/posterior polarity signals in *C. elegans*. Mol. Cell *4*, 275–280.

Stade, K., Ford, C.S., Guthrie, C., and Weis, K. (1997). Exportin 1 (Crm1p) is an essential nuclear export factor. Cell *90*, 1041–1050.

Thorpe, C.J., Schlesinger, A., Carter, J.C., and Bowerman, B. (1997). Wnt signaling polarizes an early *C. elegans* blastomere to distinguish endoderm from mesoderm. Cell *90*, 695–705.

Timmons, L., and Fire, A. (1998). Specific interference by ingested dsRNA. Nature *395*, 854.

Tzivion, G., and Avruch, J. (2002). 14-3-3 proteins: active cofactors in cellular regulation by serine/threonine phosphorylation. J. Biol. Chem. *277*, 3061–3064.

Wang, W., and Shakes, D.C. (1997). Expression patterns and transcript processing of *ftt-1* and *ftt-2*, two *C. elegans* 14-3-3 homologues. J. Mol. Biol. *268*, 619–630.